Controlling Large Fluctuations: Theory and Experiment

Mark I. Dykman and Brage Golding

Department of Physics and Astronomy, Michigan State University, East Lansing, MI 48824, USA

Abstract. We review some recent results on large infrequent fluctuations in which a system moves far away from a metastable state or makes a transition between metastable states. Although fluctuations happen at random, the motion in a large fluctuation is essentially deterministic. This makes it possible to change fluctuation probabilities exponentially strongly by comparatively weak fields, paving the way for selective control of escape rates. To investigate large fluctuations experimentally, we trap a dielectric Brownian particle in a double-well potential created by two independent optical beams. By analyzing thermal fluctuations, we can fully map the three-dimensional potential. This has allowed us to put Kramers' theory of thermally activated transitions to a quantitative experimental test. A suitable periodic modulation of the optical intensity breaks the spatio-temporal symmetry of an otherwise spatially symmetric system. This has allowed us to *localize* a particle in one of the symmetric wells.

1 Introduction

Large fluctuations, although infrequent, are responsible for big qualitative changes in various types of systems and play a crucial role in many phenomena. A well-known example of large fluctuations is thermally activated escape. It gives rise to diffusion in crystals, protein folding, and is closely related to activated chemical reactions. Fluctuating systems of interest are often far from thermal equilibrium, as in the case of lasers, pattern forming systems [1], parametrically driven trapped electrons [2], and systems which display stochastic resonance [3]. Important contributions to the theory of fluctuations in nonequilibrium systems have been made by Lutz Schimansky-Geier, to whom this book is dedicated.

Understanding large fluctuations requires theoretical and experimental study of:

- fluctuation probabilities, i.e. the probability density $p(\mathbf{q})$ for a system to occupy the state $\mathbf{q}$ far from the attractor $\mathbf{q}^{(0)}$ in phase space. For nonequilibrium systems there is no universal relation from which they can be obtained, cf. [4].
- paths along which the system moves in response to random forcing. The distribution of fluctuational paths is a characteristic of the fluctuation *dynamics*. This distribution sharply peaks at a certain *optimal path* along

J.A. Freund and T. Pöschel (Eds.): LNP 557, pp. 365–377, 2000.

which the system is most likely to move in an occasional event where it fluctuates to a vicinity of a given state $\mathbf{q}$ far from the attractor.
- response of the fluctuation probabilities to external fields. As we will see, this response is determined by the optimal paths. It may be exponentially strong and may display resonant frequency dependence. Its understanding paves the way for *controlling* fluctuations.

The fundamental role of the distribution of fluctuational paths was recognized by Onsager and Machlup [5] who obtained optimal paths for a linear Markov system in thermal equilibrium with the bath. A theory for nonlinear nonequilibrium Markov systems was developed by Wentzell and Freidlin [6] (see also [7–9]). For equilibrium systems the optimal path to a given state is the time-reversed path from this state to the stable state in the neglect of fluctuations. This is no longer true for nonequilibrium systems, because, in general, they lack time reversibility, as demonstrated in Ref. [10]. Even for simple nonequilibrium systems the pattern of optimal paths may have singular features.

Much progress has been made over the last decade in the theory of large fluctuations, and many interesting results were obtained through digital and analog simulations [11]. However, with a few important exceptions [12, 13], it was not until recently that systematic experimental work on large fluctuations has occurred [2, 14, 15]. In this article we will summarize some of the recent theoretical and experimental results.

In Sec. 2 below we present a general formulation of the problem of large fluctuations, escape from a metastable state, and optimal paths for systems driven by Gaussian noise. In Sec. 3 this formulation will be used to show that escape probabilities can be *exponentially strongly* changed by a comparatively weak ac field even if the field frequency is of the order of the relaxation rate. In Sec. 4 we describe the technique of trapping a μm-size dielectric particle in an optically created double-well potential, and provide the results of a quantitative test of the Kramers escape theory. In Sec. 5 results on interwell transitions in a periodically modulated double-well optical trap are presented. Sec. 6 contains concluding remarks.

2 Large Fluctuations Induced by Gaussian Noise

Gaussian noise is one of the most general types of noise. Therefore, within a phenomenological description of noise-induced fluctuations in dynamical systems, it is of utmost interest to analyze systems driven by Gaussian noise. A natural theoretical approach to the problem relies on the path-integral technique [8, 16–20]. We will give a closed-form formulation for a fluctuating system which is described by one dynamical variable q [21]. This formulation generalizes the results [20] for stationary systems to the case of periodically driven systems. The Langevin equation of motion is of the form:

$$\dot{q} = K(q;t) + f(t), \quad K(q;t+\tau_F) = K(q;t), \tag{1}$$

where τ_F is the period of the driving field, and $f(t)$ is a stationary Gaussian noise ("colored", in the general case). Such noise is fully characterized by the correlation function $\phi(t) = \langle f(t)f(0)\rangle$ or the power spectrum $\Phi(\omega)$ which is a Fourier transform of $\phi(t)$.

For weak noise intensities, over the noise correlation time t_{corr} and the characteristic relaxation time in the absence of noise t_{rel}, the system will approach the stable state $q^{(0)}(t)$ and will then perform small fluctuations about it. To arrive to a remote point q_f at the instant t_f, the system should have been subjected to *finite* forcing over certain time. Different realizations of the force $f(t)$ can result in the same final state, but each of them gives rise to a certain system trajectory $q(t)$ [22], which is independent of the characteristic noise intensity $D = \max\ \Phi(\omega)$. The probability density of realizations of $f(t)$ is given by the functional

$$\mathcal{P}[f(t)] = \exp\left[-\frac{1}{2D}\int dt\,dt'\, f(t)\hat{\mathcal{F}}(t-t')f(t')\right], \tag{2}$$

where $\hat{\mathcal{F}}(t)$ is a reciprocal of the noise correlation function $\phi(t)$, $\int dt_1\,\hat{\mathcal{F}}(t-t_1)\phi(t_1-t') = D\delta(t-t')$.

If the noise intensity D is sufficiently small, then for all $f(t)$ which result in a large fluctuation to a given state, the values of the functional (2) are exponentially small. For different $f(t)$, they are exponentially different. Thus one would expect that there exists a realization $f(t) = f_{\rm opt}(t)$ which is exponentially more probable than the others. This optimal realization provides the maximum to $\mathcal{P}$ subject to the *constraint* that the system (1) is driven to a designated state q_f. The path $q_{\rm opt}(t)$ along which the system moves when driven by the optimal force $f_{\rm opt}(t)$ is the optimal fluctuational path.

From (2), the paths $q_{\rm opt}$, $f_{\rm opt}$ provide the minimum to the functional

$$\begin{aligned}\mathcal{R}[q(t), f(t)] = {} & \frac{1}{2}\int\!\!\int_{-\infty}^{\infty} dt\,dt'\, f(t)\hat{\mathcal{F}}(t-t')f(t') \\ & + \int_{t_i}^{t_f} dt\,\lambda(t)\,[\dot{q} - K(q;t) - f(t)]\end{aligned} \tag{3}$$

($t_i \to -\infty$). The Lagrange multiplier $\lambda(t)$ relates the optimal paths $f_{\rm opt}(t)$ and $q_{\rm opt}(t)$ to each other.

It is straightforward to obtain from (3) the variational equations for $q_{\rm opt}(t), f_{\rm opt}(t), \lambda_{\rm opt}(t)$. Care has to be taken when the boundary conditions are discussed. In the problem of reaching the state q_f at a time t_f, they take the form

$$\begin{aligned}&f(t) \to 0 \quad \text{for} \quad t \to \pm\infty, \quad \lambda(t) \to 0 \quad \text{for} \quad t \to -\infty, \\ &\lambda(t) = 0 \quad \text{for} \quad t > t_f, \quad q(t) \to q^{(0)}(t) \quad \text{for} \quad t \to -\infty, \quad q(t_f) = q_f.\end{aligned} \tag{4}$$

The motion of the system after t_f is not important from the viewpoint of the fluctuation probability. Therefore the constraint on $f(t)$ is lifted for $t > t_f$

[20]. Clearly, the force decays to zero for $t > t_f$. However, for a non-white noise, it does not become equal to zero instantaneously.

The boundary conditions for the *escape problem* are different. Here, the optimal escape path corresponds to $q(t)$ approaching the saddle-type periodic or stationary state for $t \to \infty$, and $\lambda(t), f(t) \to 0$ for $t \to \infty$ [20].

From (2), the probability density for a system to be brought to the state q_f at t_f is of the form

$$p(q_f, t_f) \propto \exp\left[-R(q_f, t_f)/D\right], \; R(q_f, t_f) = \mathcal{R}[q_{\rm opt}, f_{\rm opt}] \equiv \min \mathcal{R}[q, f]. \quad (5)$$

The criterion of applicability of the approach is $R/D \gg 1$.

In the important case where the noise $f(t)$ is white, we have $\hat{\mathcal{F}}(t) = \delta(t)$. Therefore $f_{\rm opt}(t) = \lambda_{\rm opt}(t)$, and the variational problem (3) is reduced to the Wentzell-Freidlin functional $\bar{R}[q] = (1/2)\int dt\,[\dot{q} - K(q;t)]^2$ [6]. For K independent of t, the optimal path is given by $\dot{q}_{\rm opt} = -K(q_{\rm opt})$.

Noise color and time dependence of K make optimal paths much more complicated. Generally, the variational equation $\delta\mathcal{R} = 0$ with boundary conditions (5) has several solutions. The physically meaningful solution provides the *absolute minimum* to the functional $\mathcal{R}$. Onset of multiple solutions is signaled by vanishing of an eigenvalue of the operator $\delta^2\mathcal{R}/\delta x_i(t)\delta x_j(t)$ (x_i is q, f, λ for $i = 1, 2, 3$, respectively), which also shows where the pattern of extreme paths has *caustics*. In contrast to standard nonlinear dynamics, caustics are not encountered by "true" optimal paths which minimize R.

3 Logarithmic Susceptibility

The general formulation of Sec. 2 allows us to investigate how the probabilities of large fluctuations are changed by an external field. This is necessary for controlling fluctuations. Of utmost interest is the case where the field is *dynamically weak*, i.e. the dynamics of the system is only weakly perturbed, and in particular the number of attractors or saddle states is not changed. Yet the effect of such field on the fluctuation probability may be strong [23–25]. Of particular interest is the effect of an additive periodic force $F(t)$. In the equation of motion we set (1)

$$K(q;t) = K_0(q) + F(t), \; F(t + \tau_F) = F(t)\,. \quad (6)$$

The force $F(t)$ changes the activation energy $R(q_f, t_f)$ for reaching a state q_f (5). To the lowest order in F, the increment δR can be easily obtained from the variational formulation (3),

$$\delta R(q_f, t_f) = \int_{-\infty}^{t_f} dt\,\chi(t)F(t), \; \chi(t) = \lambda_0(t), \quad (7)$$

where $\lambda_0(t)$ is the solution of the variational problem for reaching the state q_f in the absence of the driving F.

The increment δR is *linear* in F. Even though it is small compared with R, it may be much bigger than the noise intensity D, in which case the fluctuation probability is changed by the force *exponentially strongly.* This change is fully described by the *logarithmic susceptibility* $\chi(t)$ (7) [23, 24].

The above arguments apply also to the problem of escape, in which case one should set the upper limit of integration in (7) $t_f \to \infty$. However, care has to be taken here of the fact that the optimal path for escape is an instanton. The function $\lambda_0(t)$ is other than zero in a time interval on the order of the correlation time of noise or the relaxation time of the system, and it is exponentially small otherwise. At the same time, the optimal fluctuation may occur at any time t_0, in the absence of periodic driving. The field $F(t)$ lifts this time degeneracy. It *synchronizes* optimal escape trajectories (one per period) so as to minimize the activation energy of escape. Therefore one may expect that the change of the escape activation energy

$$\delta R_{\text{escape}} = \min_{t_0} \int_{-\infty}^{\infty} dt\, \chi(t - t_0) F(t). \tag{8}$$

A derivation for white-noise driven systems is given in [24].

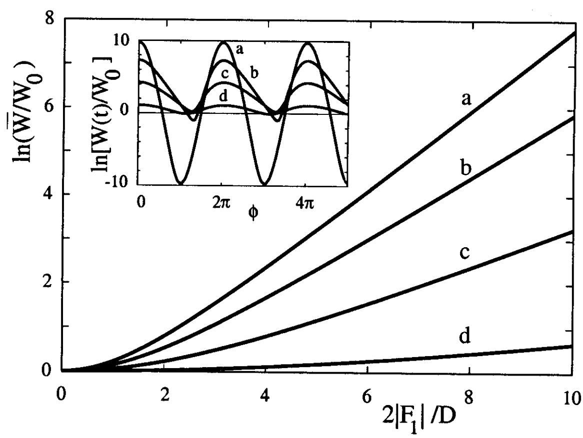

Fig. 1. The logarithm of the time-average escape rate $\bar{W}$ as a function of the scaled amplitude $2|F_1|/D$ of the driving field $F(t) = 2\mathrm{Re}\,[F_1 \exp(i\omega_F t)]$ for an overdamped Brownian particle. The curves a to d refer to the dimensionless frequency $\omega_F = 0.1, 0.4, 0.7, 1.2$, and $K_0(q) = -q + q^2$ in Eq. (6). Inset: time dependence of the logarithm of the instantaneous escape rate for the same frequencies and $2|F_1|/D = 10$ ($\phi = \omega_F t$), illustrating loss of synchronization of escape events with increasing ω_F (optimal escape paths remain synchronized) [25]

The increment (8), although linear in the field amplitude, is essentially *nonanalytic* in the field. A counterintuitive feature of this expression is that the escape rate is modified exponentially strongly even where the field frequency largely exceeds the escape rate. This is qualitatively different from the situation considered in "conventional" stochastic resonance, where the analysis is limited to the low-frequency adiabatic modulation, and the escape rate is determined by the instantaneous barrier height.

Using the logarithmic susceptibility, one can find not only the exponent, but also the prefactor in the escape rate, and thus obtain a *complete nonadiabatic solution* of the escape problem for an overdamped periodically driven system [25]. The prefactor problem has attracted much attention since the Kramers paper [26] where it was considered for systems in thermal equilibrium. Much work was done to generalize the Kramers results to nonequilibrium Markov systems ([27] and references therein). A driven overdamped system is the prototypical nonequilibrium system where an explicit solution was obtained both for the exponent and the prefactor [25]. We note that the technique [25] can be generalized to other systems where escape occurs over an unstable limit cycle.

The explicit solution [25] shows how the time dependence of the instantaneous escape rate $W(t)$ varies with field frequency ω_F. For small ω_F, the time dependence of $W(t)$ is exponentially strong, $W \propto \exp[-\kappa F(t)/D]$ where $\kappa = \int dt\, \chi(t)$. For higher field frequencies, it becomes much weaker, as seen from Fig. 1.

4 Testing Kramers' Theory of Escape

A simple physical system which embodies fluctuation-induced escape is a mesoscopic particle suspended in a liquid and confined within a metastable potential well. The particle moves at random within the well until a large fluctuation propels it over an energy barrier. An optically transparent dielectric sphere can be readily trapped with a strongly focused laser beam, creating an optical gradient trap, i.e. "optical tweezers" [28]. Techniques based on optical tweezers have found broad applications in contactless manipulation of objects such as atoms, colloidal particles, and biological materials. Fluctuation-induced escape can be studied using a dual optical trap generated by two closely spaced parallel light beams, as illustrated in Fig. 2. Such trap was implemented initially to study the synchronization of interwell transitions by periodic forcing [29].

A particle in a double-well trap can be used to understand transition rates in a stationary potential, and thus to provide a rigorous test of the multidimensional Kramers rate theory with no adjustable parameters. It can also be used to investigate transition rates in an ac-modulated potential. Quantitative measurements require that the confining potential be adequately characterized and under the control of the experimentalist.

In our experiment [14], each of the two focussed beams produces a stable three-dimensional trap as a result of electric field gradient forces exerted on a transparent dielectric spherical silica particle of diameter $2R = 0.6$ μm.

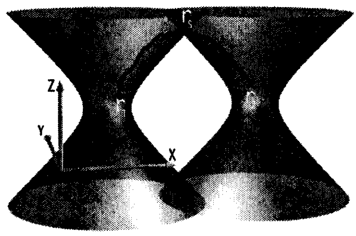

Fig. 2. Rendering of two focused laser beams, the equilibrium positions of the particle (rings), and a transitional path between the beams

Displaced typically by 0.25 to 0.45 μm, the beams create a double-well potential, with the stable positions of the particle center at $\mathbf{r}_1$ and $\mathbf{r}_2$. The stability perpendicular to the beam axis is due to the Gaussian transverse beam profile gradient; in the beam direction the potential gradient is derived from the strong focusing of the objective lens [28]. Relatively infrequent thermally activated random transitions between the potential wells occur through a saddle point at $\mathbf{r}_s$ as depicted in Fig. 2. The experimental setup is discussed elsewhere [14].

The experimental outputs are the three spatial coordinates of the center of the particle sampled at 5 ms intervals $\mathbf{r}(t_i)$. The particle spends most of its time in the vicinity of the stable points $\mathbf{r}_1$ and $\mathbf{r}_2$ with infrequent transitions between them. As a result of the short equilibration time of the sphere in water ($\gamma^{-1} = M/6\pi\eta R \sim 10^{-7}$ s, where η is the viscosity of water and M is the particle mass), the velocity of the Brownian particle relaxes to equilibrium on a scale much shorter than the sampling time. The stationary spatial probability density is

$$\rho(\mathbf{r}) = Z^{-1} \exp[-U(\mathbf{r})/k_B T] . \tag{9}$$

Eq. (9) enables us to *compute*, from the observations of the particle fluctuations, the full three-dimensional confining potential $U(\mathbf{r})$. Results for a particular two-beam trap are shown in Fig. 3. We choose the x axis to be in the direction from one beam to the other and the z axis along the beams' propagation direction. The potential minima, $\mathbf{r}_1$ and $\mathbf{r}_2$, lie in the symmetry plane $y = 0$ formed by the beam axes. Fig. 3a shows a 2-dimensional cross-section, at $y = 0$, of the potential with energy contours at 1.0 $k_B T$ intervals, distinguished by differing shading. If, for a given x, we find the minimum of $U(\mathbf{r})$ over y and z, we obtain the familiar one-dimensional representation of a double-well potential shown in Fig. 3b. In the y-direction, the potential has only one well, as seen from Figs. 3c,d.

The striking feature of the effective potential evident in Fig. 3a is the strong symmetry breaking about the focal plane, which is the symmetry plane of the beams, unperturbed by the particle. The symmetry breaking leads to the single saddle point in $U(\mathbf{r})$ instead of two saddle points as might be inferred from Fig. 2. This aspect of the potential is not an artifact of specific experimental conditions, such as non-parallel optical beams, but is a consequence of the beam-particle interaction. The dielectric particle acts as a spherical lens to refocus the beam inside the sphere. When the particle is displaced in the $+z$ direction above the focal plane, the electromagnetic field is most strongly "squeezed" into the particle, thus minimizing the free energy of the polarized particle in the field.

In the vicinity of $\mathbf{r}_1$, $\mathbf{r}_2$, and $\mathbf{r}_s$, the potential $U(\mathbf{r})$ is quadratic in the displacements $\delta\mathbf{r} = \mathbf{r} - \mathbf{r}_i$ with $i = 1, 2, s$. In order to obtain the eigenvalues $|\omega_i|^2$ of the corresponding quadratic form for a given potential, we performed a least-squares fit to the data in the vicinity of $\mathbf{r}_i$. The characteristic frequencies $|\omega_i|$ are small compared to the damping rate γ, so the particle is overdamped.

A quantitative description of thermally activated escape from a one-dimensional metastable potential was given by Kramers [26] and subsequently extended to multidimensional potentials [30]. For an overdamped Brownian particle in a potential $U(\mathbf{r})$, the Kramers transition rate is

$$W^K = W_0^K \exp\left(-\Delta U / k_B T\right), \quad W_0^K = \frac{|\omega_s^{(1)}| \omega^{(1)}}{2\pi\gamma} \frac{\omega^{(2)}\omega^{(3)}}{\omega_s^{(2)}\omega_s^{(3)}}, \tag{10}$$

where ΔU is the height of the potential barrier, whereas $\omega_s^{(j)}$ and $\omega^{(j)}$ characterize, respectively, the curvatures of the potential at the saddle point and at the minimum from which the system escapes, in the normal jth directions, with $(\omega_s^{(1)})^2 < 0$. Therefore, with knowledge of the potential, not only the exponential term, but also the prefactor can be explicitly computed.

Eq. (10) was tested by systematically varying ΔU. The transition rates W^{meas} were obtained from the mean dwell time in each state (or by fitting an exponential to a histogram of dwell times) as a function of $\Delta U/k_B T$. The data demonstrate the Arrhenius-like character of the rates. A more definitive test is shown in Fig. 4. Here, the Kramers rates, W^K , calculated from Eq. (10) using the experimentally determined curvatures, are plotted along the vertical axis vs. W^{meas} on the horizontal axis. The solid line of slope one denotes the coincidence of theory and experiment. The data fall remarkably close to the line, yielding a striking confirmation of the multidimensional Kramers theory of transition rates [26].

5 Dynamical Symmetry Breaking and ac–Induced Localization of a Particle

We now discuss observations on modulation of escape rates by an ac-field. The effect is particularly interesting for a particle in a spatially periodic potential, as it gives rise to *directed diffusion* [31]. It follows from the results of Sec. 3

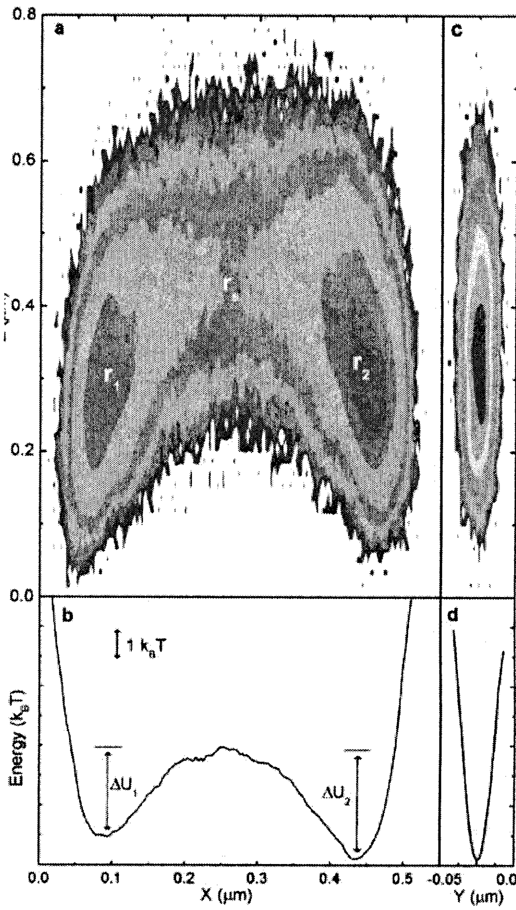

Fig. 3. The potential energy of the particle in the double-well trap as determined by experiment. (a) Energy contours for a cross-section in the $x-z$ plane containing the two stable points and the saddle point. (b) The energy, minimized with respect to y and z, as a function of x. (c) Same as in (a), but in the $y-z$ plane. (d) The energy, minimized with respect to x and z, as a function of y [14].

that, for a generic periodic potential, an ac field performs more work on the particle as it moves along the optimal escape path in one direction than in the other, thereby more strongly reducing the corresponding potential barrier and producing diffusion in that direction.

An effect closely related to directed diffusion but more amenable to testing using optical trapping is ac-field induced localization in one of the wells of a symmetric double-well potential. We expect both these effects to occur if the applied field breaks the spatio-temporal symmetry of the system [23, 32–34]. The ratio of the stationary populations w_1, w_2 of the wells is determined by

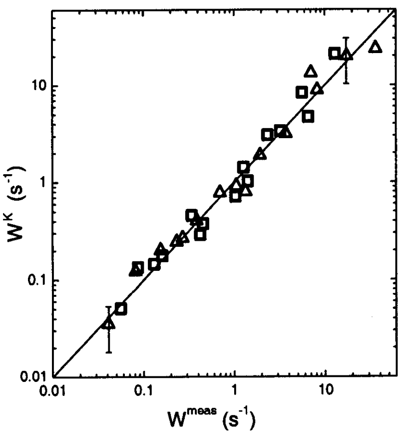

Fig. 4. Comparison of the measured transition rates W^{meas} and the rates calculated from the three-dimensional Kramers theory, W^K, using the measured curvatures of the potential wells. The squares represent escapes from the well at $\mathbf{r}_1$ and the triangles represent escapes from the well at $\mathbf{r}_2$. The line of slope one indicates the result expected if the three-dimensional Kramers theory correctly predicted the measured transition rates [14]

the ratio of the rates W_{ij} of the interwell transitions,

$$w_1/w_2 = W_{21}/W_{12} \propto \exp([\delta(\Delta U_1) - \delta(\Delta U_2)]/k_B T), \tag{11}$$

where $\delta(\Delta U_{1,2})$ are field-induced corrections to the activation energies of escape from the wells 1,2, which are given by (8).

The experiment is conducted by setting the static barrier height $\Delta U_1 = \Delta U_2 \equiv \Delta U_0 \approx 8k_BT$. Optical intensity of a beam is then modulated by an electro-optic device, giving rise to modulation of the reduced barrier height $\Delta U/k_BT$ with an amplitude ≈ 2.5. The modulation frequency $\omega/2\pi$ is varied between 1 to 100 Hz. This may be compared to the mean unmodulated transition rate $W \sim 0.1\mathrm{s}^{-1}$. The form of the modulation is $\Delta U(t) = \Delta U_0 + A[\sin(\omega t) + (1/2)\sin(2\omega t + \phi)]$. A useful feature of this waveform is the presence of the control parameter ϕ. As shown in the insets to Fig. 5, the sign of the barrier height shift during the first part of the cycle can be inverted between left and right hand wells if the phase angle is shifted by π. The potential is not invariant under $t \to t + \pi/\omega, \mathbf{r} \to -\mathbf{r}$ (with $\mathbf{r}$ measured from the inversion center in the absence of modulation), and this leads to breaking of the spatial symmetry over a cycle of the modulation.

The modulation of the escape rates results in unbalanced averaged occupation probabilities of the left and right wells. In the experiment, they differ by 20% for the modulation amplitude used. This is sufficient to create significant directional diffusion, and demonstrates onset of *dynamical* symmetry breaking.

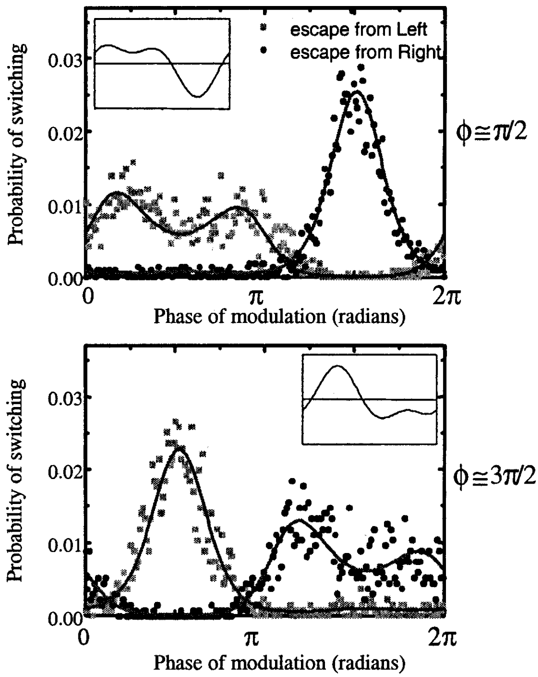

Fig. 5. Plots of the time-dependent switching probabilities out of a double-well potential over a cycle ωt of the modulating waveform. The upper and lower panels show the role of the phase angle ϕ in controlling the transition rates. Solid lines show the theoretical results based on Eq. (8). Insets show the instantaneous difference between the heights of the potential barriers in the two wells.

6 Conclusions

In summary, we have shown how to describe the dynamics of large fluctuations. It follows from the results that the response of fluctuation probabilities to an ac-field can be described in a fairly universal way using the notion of logarithmic susceptibility. Even where this quantity may not be calculated, it can be measured experimentally and then used for selective control of fluctuations. We have also shown that thermal fluctuations can be used to measure the complete confining potential of a particle in an optical trap. Our results provide a direct quantitative confirmation of the full three-dimensional Kramers theory of transition rates, throughout a broad range of barrier heights and potential well shapes, measured independently. By modulating the barrier height with a weak biharmonic waveform, the particle can be induced to favor occupying a particular well in a symmetric double-well potential. This dynamic symmetry breaking is readily controlled by manipulation of the relative phase of the two components of the waveform.

Acknowledgments

We are grateful to Lowell McCann and Vadim Smelyanskiy with whom many of the results discussed in this paper were obtained. This research was partly supported by the NSF through Grants PHY-9722057 and DMR-9971537.

References

1. Cross M.C. and Hohenberg P.C. (1993) Pattern-formation outside of equilibrium, Rev. Mod. Phys. **65**, 851–1112; Haken H. (1993) Advanced Synergetics, Springer, Berlin
2. Lapidus L.J., Enzer D., and Gabrielse G. (1999) Stochastic phase switching of a parametrically driven electron in a Penning trap, Phys. Rev. Lett. **83**, 899
3. Schimansky-Geier L, et al. (1998) Noise induced order: Stochastic resonance, Int. J Bifurcat Chaos **8**, 869
4. Schimansky-Geier L. and Zülicke Ch. (1990) Harmonic noise: Effect on bistable systems. Z. Phys. B **79**, 451–460
5. Onsager L. and Machlup S. (1953) Fluctuations and irreversible processes, Phys. Rev. **91**, 1505
6. Freidlin M.I. and Wentzell A.D. (1984) Random Perturbations in Dynamical Systems. Springer, New York
7. Graham R (1989) Macroscopic potentials, bifurcations and noise in dissipative systems. In: Moss F. and McClintock P.V.E. (Eds) Noise in Nonlinear Dynamical Systems. Cambridge University Press, Cambridge, vol. 1, 225–278
8. Dykman M.I., Krivoglaz M.A., and Soskin S.M. (1989) Transition probabilities and spectral densities of fluctuations of noise-driven bistable systems. In: Moss F. and McClintock P.V.E. (Eds) Noise in Nonlinear Dynamical Systems. Cambridge University Press, Cambridge, vol. 2, 347–380
9. Maier M.S. and Stein D.L. (1996) A scaling theory of bifurcations in the symmetric weak-noise escape problem. J. Stat. Phys. **83**, 291–357
10. Luchinsky D.G. and McClintock P.V.E. (1997) Irreversibility of classical fluctuations studied in analogue electrical circuits, Nature **389**, 463–466
11. Luchinsky D.G., McClintock P.V.E., and Dykman M.I. (1998) Analogue studies of nonlinear systems. Rep. Progr. Phys. **61**, 889–997
12. Devoret M.H. et al. (1987) Resonant activation of a Brownian particle out of a potential well: Microwave-enhanced escape from the zero-voltage state of a Josephson junction. Phys. Rev. B **36**, 58–73; Turlot E. et al. (1998) High-frequency satellites in resonant activation. Chem. Phys. **235**, 47–50
13. Han S., Lapoint J., and Lukens J.E. (1992) Effect of a two-dimensional potential on the rate of thermally induced escape over the potential barrier. Phys. Rev. B **46**, 6338–6345
14. McCann L.I., Dykman M.I., and Golding B. (1999) Thermally activated transitions in a bistable three-dimensional optical trap. Nature **402**, 785–787
15. Hales J. et al. (2000) Dynamics of activated escape and its observation in a semiconductor laser. cond-mat/0002036
16. Luciani J.F. and Verga A.D. (1987) Functional integral approach to bistability in the presence of correlated noise. Europhys. Lett. **4**, 255

17. Bray A.J. and McKane A.J. (1989) Instanton calculation of the escape rate for activation over a potential barrier driven by colored noise. Phys. Rev. Lett. **62**, 493–496; McKane A.J. (1989) Noise-induced escape rate over a potential barrier: results for general noise. Phys. Rev. A **40**, 4050–4053
18. Förster A. and Mikhailov A.S. (1988) Optimal fluctuations leading to transitions in bistable systems Phys. Lett. A **126**, 459–62
19. Wio H.S. et al. (1989) Path-integral formulation for stochastic processes driven by colored noise. Phys. Rev. A **40**, 7312–24
20. Dykman M.I. (1990) Large fluctuations and fluctuational transitions in systems driven by colored Gaussian noise: A high-frequency noise. Phys. Rev. A **42**, 2020–2029
21. Dykman M.I. (2000) Nonlinear dynamics of large fluctuations, and how it can be controlled. In: Broomhead D.S. et al. (Eds) Stochastic and Chaotic Dynamics in the Lakes. AIP Conference Proceedings **502**, Melville, p. 3–13
22. Feynman R.P. and Hibbs A.R. (1965) Quantum Mechanics and Path Integrals. McGraw-Hill, New York
23. Dykman M.I. et al. (1997) Resonant directed diffusion in nonadiabatically driven systems. Phys. Rev. Lett. **79**, 1178–81
24. Smelyanskiy V.N. et al. (1997) Fluctuations, escape, and nucleation in driven systems: logarithmic susceptibility. Phys. Rev. Lett. **79**, 3113–16
25. Smelyanskiy V.N., Dykman M.I., and Golding B. (1999) Time oscillations of escape rates in periodically driven systems. Phys. Rev. Lett. **82**, 3193–3196
26. Kramers H. (1940) Brownian motion in a field of force and the diffusion model of chemical reactions. Physica (Utrecht) **7**, 284–304
27. Maier R.S, and Stein D.L. (1997) Limiting exit location distributions in the stochastic exit problem. SIAM J. Appl. Math. **57**, 752-790
28. Ashkin A. et al. (1986) Observation of a single-beam gradient force optical trap for dielectric particles. Optics Lett. **11**, 288–291
29. Simon A. and Libchaber A. (1992) Escape and synchronization of a Brownian particle. Phys. Rev. Lett. **68**, 3375–3378
30. Landauer R. and Swanson J.A. (1961) Frequency factors in the thermally activated process. Phys. Rev. **121**, 1668–1674
31. Magnasco M. (1993) Forced thermal ratchets. Phys. Rev. Lett. **71**, 1477–80
32. Ajdari A. et al. (1994) Rectified motion-induced by ac forces in periodic structures. J. Phys. I (France) **4**, 1551–61
33. Mahato M.C. and Jayannavar A.M. (1994) Synchronized first-passages in a double-well system driven by an asymmetric periodic field. Phys. Lett. A **209**, 21–5
34. Chialvo D.R. and Millonas M.M. (1995) Asymmetric unbiased fluctuations are sufficient for the operation of a correlation ratchet. Phys. Lett. A **209**, 26–30